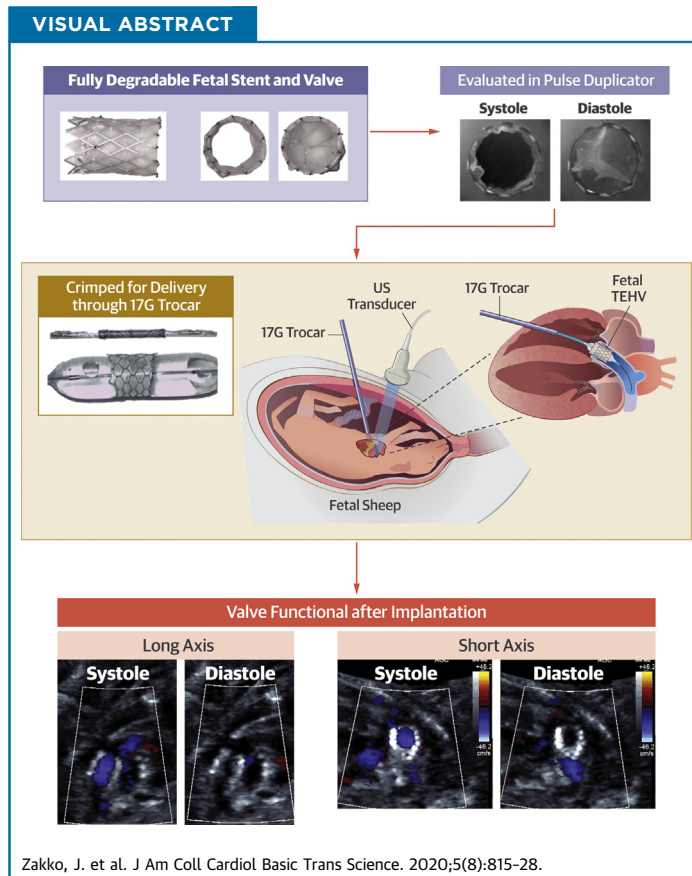


PRECLINICAL RESEARCH

# Development of Tissue Engineered Heart Valves for Percutaneous Transcatheter Delivery in a Fetal Ovine Model



Jason Zakko, MD, MS,<sup>a,b,\*</sup> Kevin M. Blum, MS,<sup>a,c,\*</sup> Joseph D. Drews, MD, MS,<sup>a,b,\*</sup> Yen-Lin Wu, MS,<sup>d,\*</sup> Hoda Hatoum, PhD,<sup>e,\*</sup> Madeleine Russell, BS,<sup>f,\*</sup> Shelley Gooden, MS,<sup>e</sup> Megan Heitkemper, MS,<sup>a,c</sup> Olivia Conroy, BS,<sup>f</sup> John Kelly, MD,<sup>a,g</sup> Stacey Carey, RN,<sup>g</sup> Michael Sacks, PhD,<sup>f,†</sup> Karen Texter, MD,<sup>g,†</sup> Ellie Ragsdale, MD,<sup>h,†</sup> James Strainic, MD,<sup>i,†</sup> Martin Bocks, MD,<sup>j,†</sup> Yadong Wang, PhD,<sup>d,†</sup> Lakshmi Prasad Dasi, PhD,<sup>e,†</sup> Aimee K. Armstrong, MD,<sup>g,†</sup> Christopher Breuer, MD<sup>a,b,†</sup>



From the <sup>a</sup>Center for Regenerative Medicine, Abigail Wexner Research Institute at Nationwide Children's Hospital, Columbus, Ohio; <sup>b</sup>Department of Surgery, Ohio State University Wexner Medical Center, Columbus, Ohio; <sup>c</sup>Department of Biomedical Engineering, Ohio State University, Columbus, Ohio; <sup>d</sup>Meinig School of Biomedical Engineering, Cornell University, Ithaca, New York; <sup>e</sup>Coulter Department of Biomedical Engineering, Georgia Tech, Atlanta, Georgia; <sup>f</sup>Oden Institute for Computational and Engineering Sciences, University of Texas at Austin, Austin, Texas; <sup>g</sup>Heart Center, Nationwide Children's Hospital, Columbus, Ohio; <sup>h</sup>Department of OB/GYN-Maternal Fetal Medicine, University Hospitals Cleveland Medical Center, Cleveland, Ohio; <sup>i</sup>Department of Pediatric Cardiology, University Hospitals Rainbow Babies and Children's Hospital, School of Medicine,

## ABBREVIATIONS AND ACRONYMS

**EOA** = effective orifice area

**M<sub>n</sub>** = molecular size

**MPA** = main pulmonary artery

**M<sub>w</sub>** = molecular weight

**NOI** = normalized orientation index

**PCL** = polycaprolactone

**PDI** = polydispersity index

**PG** = pressure gradient

**RF** = regurgitant fraction

**RV** = right ventricular/ventricle

**SEM** = scanning electron microscopy

**TEHV** = tissue-engineered heart valve

## SUMMARY

This multidisciplinary work shows the feasibility of replacing the fetal pulmonary valve with a percutaneous, transcatheter, fully biodegradable tissue-engineered heart valve (TEHV), which was studied in vitro through accelerated degradation, mechanical, and hemodynamic testing and in vivo by implantation into a fetal lamb. The TEHV exhibited only trivial stenosis and regurgitation in vitro and no stenosis in vivo by echocardiogram. Following implantation, the fetus matured and was delivered at term. Replacing a stenotic fetal valve with a functional TEHV has the potential to interrupt the development of single-ventricle heart disease by restoring proper flow through the heart. (J Am Coll Cardiol Basic Trans Science 2020;5:815-28) © 2020 The Authors. Published by Elsevier on behalf of the American College of Cardiology Foundation. This is an open access article under the CC BY-NC-ND license (<http://creativecommons.org/licenses/by-nc-nd/4.0/>).

Congenital cardiac anomalies represent the most common birth defect, affecting approximately 0.9% of all live births (1). Despite significant advances in surgical and medical management, they remain a leading cause of death in the newborn period and lead to lifelong morbidity in survivors (1). Most major congenital cardiac anomalies require reconstructive surgery, often requiring the use of man-made, xenographic, or homograft material in the form bioprosthetic heart valves and valved conduits. Use of these valves and conduits is a significant source of morbidity and reoperations, owing to biocompatibility issues (2). For example, bioprosthetic valves and conduits are subject to conduit contracture and shrinkage, tissue degeneration, calcification, immunologic response consistent with cellular rejection, and somatic outgrowth, leading to the need for multiple valve replacements (3). This is particularly true for valve replacements in young children. When valved conduits are implanted in infants and young children, the median time to the next conduit replacement is only 7.5 years, and right ventricular (RV) outflow tract reconstructions in patients under 2 years of age have a 5-year freedom from intervention of 46.1%, demonstrating a need for improved valves for these patients (4,5).

Tissue engineering provides a potential strategy for creating better biomaterials for use in

reconstructive cardiac operations. Using tissue engineering techniques, replacement heart valves can be made from a biodegradable scaffold and an individual's own cells. Over time, the resulting autologous neovalves become living structures with the ability to grow, repair, and remodel. The regenerative capacity of the fetal milieu makes it a prime target for tissue regeneration and neovalve formation. This unique environment was the impetus for the development of fetal cardiac interventions. Fetal pulmonary balloon valvuloplasty is performed in fetuses with pulmonary atresia and intact ventricular septum or near-pulmonary atresia and intact ventricular septum in an attempt to allow the right heart to remodel enough to support a biventricular circulation after birth (6). However, of 21 fetuses who underwent technically successful or partially successful fetal interventions, almost all had restenosis during later gestation, and 4 had reatresia (6). Fetal pulmonary valve replacement has the potential to prevent restenosis and reatresia from occurring. Weber et al. (7) implanted 9 tissue-engineered heart valves (TEHVs) sewn into self-expanding nitinol stents and delivered into the ovine fetal pulmonary annulus through a fetal thoracotomy and purse-string suture in the RV using a 14-F (4.7 mm) delivery system. Nitinol does not have growth capacity and needs a large-profile delivery system, requiring uterine and fetal incisions. A fully bioabsorbable

Case Western Reserve University, Cleveland, Ohio; and the <sup>1</sup>University Hospitals Rainbow Babies and Children's Hospital, School of Medicine, Case Western Reserve University, Cleveland, Ohio. \*Drs. Zakko, Blum, Drews, Wu, Hatoum, and Russell contributed equally to this work and are joint first authors. †Drs. Sacks, Texter, Ragsdale, Strainic, Bocks, Wang, Dasi, Armstrong, and Breuer contributed equally to this work and are joint senior authors. This work was supported by TL1TR001069 (to Dr. Zakko), T32HL098039 (to Dr. Kelly), and TL1TR002735 (to Ms. Heitkemper). The authors have reported that they have no relationships relevant to the contents of this paper to disclose.

The authors attest they are in compliance with human studies committees and animal welfare regulations of the authors' institutions and Food and Drug Administration guidelines, including patient consent where appropriate. For more information, visit the *JACC: Basic to Translational Science* [author instructions page](#).

Manuscript received March 30, 2020; revised manuscript received June 10, 2020, accepted June 10, 2020.

stent for valve delivery is needed to allow growth and remodeling with the patient throughout fetal life and childhood.

We sought to construct the first completely bioabsorbable TEHV for fetal percutaneous and transcatheter implantation in the pulmonary valve position. We modeled the TEHV after currently available transcatheter techniques for replacing pulmonary and aortic valves in children and adults (8,9). In this manner, balloon-expandable valves are sewn into a stent, crimped onto an angioplasty balloon, and delivered through a catheter into the existing degenerated valve. Inflation of the angioplasty balloon expands the stent within the valve annulus, thereby pinning the existing degenerated leaflets between the stent and the annulus. Despite its technical challenges, the development of a percutaneous, transcatheter delivery system for TEHV replacement in utero would be superior to utilization of open fetal surgical methods, owing to the lower incidence of inducing labor using minimally invasive methods compared with open methods, as well as obviating the need for uterine and fetal incisions (10). In this work, we present a multidisciplinary approach to develop a completely bioabsorbable TEHV that is delivered through a percutaneous and transcatheter approach to the fetal pulmonary annulus in a large animal model.

## METHODS

**STENT DEVELOPMENT.** In order to create the completely bioabsorbable structure, a bioabsorbable metal alloy stent was used, which was previously shown in a rabbit model to be an excellent bioabsorbable stent material candidate (11). A zinc-aluminum alloy of 96% zinc and 4% aluminum (Zn-4Al) was used to manufacture the stents. Zn-4Al ingots were cast at Michigan Tech University (Houghton, Michigan) and placed under a repetitive thermal processing to achieve the desirable fine alloy microstructure (Fort Wayne Medical, Fort Wayne, Indiana). The ingots were then extruded into ~12-mm rods, which were machined to 10 mm in length. The rods were then drawn into 1.8-mm outer diameter tubes with an average wall thickness of 0.151 mm. The tubes were laser cut into a proprietary closed-cell stent design to minimize stress and strain during balloon inflation. The stents were electropolished and sterilized with low-temperature ethylene oxide gas. The estimated foreshortening at an inflation diameter of 7 mm was ~20%, with resulting final length of ~8 mm following deployment.

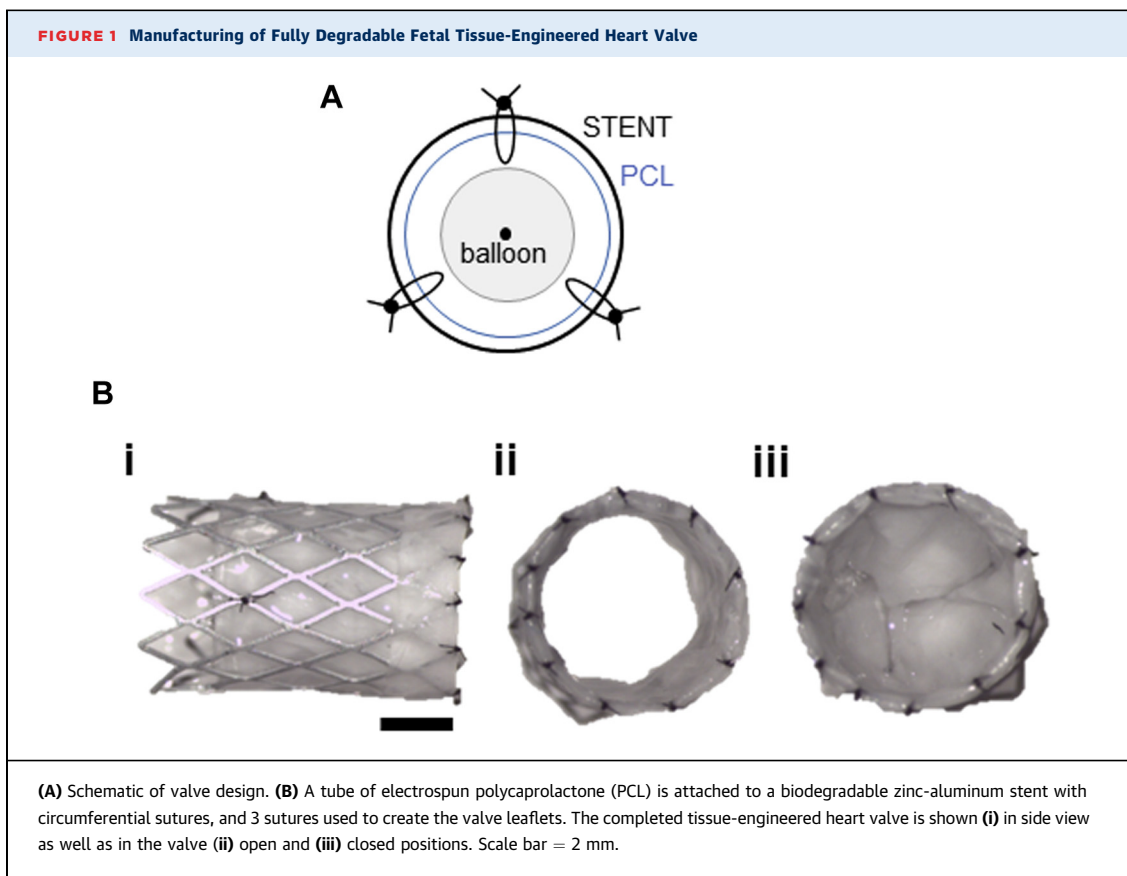
**ELECTROSPINNING.** The valves were constructed of electrospun polycaprolactone (PCL) (molecular size  $[M_n] = 80,000$  Da) (Sigma-Aldrich, St. Louis, Missouri). Electrospinning solution was prepared by dissolving PCL in an aqueous 2,2,2-trifluoroethanol (Sigma-Aldrich) mixture (volume ratio of 2,2,2-trifluoroethanol to deionized water = 5 to 1) at 14 wt/vol%. PCL was electrospun onto a rotating mandrel (6.35-mm diameter) wrapped with aluminum foil (Boardwalk Essendant, Deerfield, Illinois), using the following conditions: applied voltage =  $\pm 12$  kV, needle size = 22 gauge, distance between needle and aluminum collector = 30 cm, distance between the mandrel and aluminum collector = 10 cm, PCL solution infusion velocity = 29  $\mu\text{l}/\text{min}$ , mandrel angular speed = 80 rpm. The thickness of the PCL tubular scaffold was controlled in a targeted range of 50 to 100  $\mu\text{m}$  by measuring the mandrel under high-speed laser micrometer (LS-7070M; Keyence Corp., Itasca, Illinois) (12).

**TEHV CONSTRUCTION IN THE STENT.** To construct the TEHV in the zinc stent, the electrospun PCL tube was fashioned into a valved-conduit using a tube-within-a-tube technique (13). The stent was first expanded using a commercially available low profile 6 mm balloon catheter. A 6 mm  $\times$  8 mm PCL tube was then placed in the stent lumen and positioned within the proximal two-thirds of the stent. Using a 10-0 monofilament suture, the PCL tube was attached to the proximal end of the stent with interrupted stitches circumferentially. The PCL was then sutured in 3 locations inside of the zinc stent to form a biodegradable trileaflet TEHV (Figure 1).

**VALVE STRUCTURAL CHARACTERIZATION.** ImageJ 2.0.0 (National Institutes of Health, Bethesda, Maryland) and an image analysis-based structural characterization algorithm previously developed (14) were used to characterize the PCL fiber network. Scanning electron microscopy (SEM) images of 500 $\times$  (n = 7) and 1000 $\times$  (n = 7) were analyzed and fibrous mesh characteristics including fiber tortuosity, alignment and density were quantified. Tortuosity was measured using ImageJ through tracing the total and end-to-end fiber lengths of a representative 12 fibers in each SEM image, with tortuosity calculated as:

$$\text{Tortuosity } (\tau) = \frac{\text{Total Fiber Length}}{\text{End to End Fiber Length}}$$

For fiber alignment, the normalized orientation index (NOI) was chosen as a representative measurement and was calculated using the previously



mentioned structural characterization algorithm. An NOI is defined as:

$$NOI = \frac{90 - OI}{90} * 100\% , NOI \in [0\% 100\%]$$

where the OI (orientation index) is defined as the angle range containing the orientation of 50% of all fibers (14). The algorithm calculates NOI by creating a skeletonization of the fibers in the mesh, measuring the orientation angle of each fiber detected, and calculating an orientation distribution function. The OI is then calculated as the angle range containing half of all fibers centered on the main angle of orientation. After normalization, the NOI represents a single value corresponding to fiber alignment, with an NOI value of 0% representing no fiber alignment and 100% representing very high fiber alignment.

Linear fiber density was calculated from SEM images at 1,000 $\times$  magnification using the structural characterization code as:

$$\xi = \frac{\text{Total Fiber Length}}{\text{Total Area}}$$

**ACCELERATED DEGRADATION.** Dried samples of the electrospun PCL underwent accelerated degradation testing by using a high-pH solution to

accelerate the natural hydrolysis degradation mechanism of the PCL polymer. The samples were massed, rinsed in 100% ethanol, and submerged in 1-ml vials of 6-M sodium hydroxide at room temperature. At the end of the degradation time, samples were rinsed twice with dH<sub>2</sub>O, frozen to -80°C, and lyophilized overnight. Dry masses at the end of degradation were compared with pre-degradation masses to determine remaining mass, and samples were then processed for scanning electron microscopy or gel permeation chromatography.

**GEL PERMEATION CHROMATOGRAPHY.** The changes of molecular weight distributions of the PCL scaffold through the accelerated degradation duration were characterized by gel permeation chromatography (OMNISEC GPC/SEC system; Malvern Panalytical, Malvern, United Kingdom), equipped with a light scattering detector and differential refractive index detector. A single-pore column with 70,000-Da exclusion limit and a general-purpose mixed-bed column with 20,000,000-Da exclusion limits (Viscotek T-3000 and D-6000M, 300  $\times$  8.0 mm dimensions; Malvern Panalytical) were used for separation, along with tetrahydrofuran used as stationary and mobile phases, respectively. A total of 1 mg/ml of each

polymer sample in tetrahydrofuran solution was prepared and filtered through a 0.2- $\mu\text{m}$  syringe filter before testing. Polystyrene was used as a standard for molecular weight calibration with a concentration of 1 mg/ml. Weight average molecular weight ( $M_w$ ), number average  $M_n$ , and polydispersity index (PDI), a measure of the heterogeneity within the sample defined as  $M_w/M_n$ , were evaluated using OMNI-SEC software.

**SCANNING ELECTRON MICROSCOPY.** Samples were mounted on SEM mounts using double-sided carbon tape, and sputter coated with gold under Argon gas to 3 nm. Samples were then imaged on a Hitachi S4800 SEM (Hitachi, Tokyo, Japan) at 5 kV.

**BIAXIAL MECHANICAL TESTING.** To perform the biaxial testing,  $5 \times 5$  mm specimens were excised and mounted in an orientation perpendicular to the axial direction of the PCL tube. A  $2 \times 2$  array of small, black markers, measuring approximately 50 to 150  $\mu\text{m}$  in diameter, were used to mark each specimen in the central  $1 \times 1$  mm region of the specimen. The markers were applied on the specimens using a STAEDTLER pigment lining pen (STAEDTLER, Nuremberg, Germany). All testing occurred in deionized water at room temperature. Each specimen underwent 9 test protocols. For each protocol, a prescribed deformation was applied to the specimen using 12 independent actuators. The markers were used to measure the deformation gradient and provide feedback to the control system. Six load cells were used to capture force measurements as the specimen was deformed. The resulting first Piola-Kirchhoff stress tensor was calculated for each protocol. The material's response to deformations was determined using 9 protocols. First, the material's response to axial deformations was characterized. In the first protocol, a constant equibiaxial ratio of deformation was applied ( $F_{11}:F_{22}$ ) = 1.1:1.1 for 10 cycles. The next 4 protocols applied 5 cycles of axial deformation of varying ratios of  $F_{11}$  to  $F_{22}$  equal to 1.033:1.1, 1.02:1.1, 1.1:1.033, and 1.1:1.02, respectively. Next, the material's response to shear deformations was characterized. Three protocols applied 5 cycles of different types of shear deformation equal to -0.15 in the  $F_{12}$ ,  $F_{21}$ , and  $F_{12}$  and  $F_{21}$  directions, respectively. This allowed for a broad characterization of the shear response of the specimens. Finally, the last protocol applied both maximum biaxial deformation and shear deformation:  $F_{11} = F_{22} = 1.1$  and  $F_{12} = F_{21} = -0.15$ . Images were taken of the specimen both before and after testing to observe any inelastic effect on the material due to the mechanical testing.

**HEMODYNAMIC ASSESSMENT.** A hemodynamic evaluation of the prototype TEHV was performed using a dedicated right heart pulse duplicator, similar to previous studies (15-17). Briefly, the pulse duplicator was composed of a reservoir to mimic atrial function, a bladder pump controlled by compressed air to simulate ventricular function, and a mechanical valve between the reservoir and the pump that functioned as an atrioventricular valve. The duplicator also included a pulmonary valve chamber with an annulus of 8 mm, where the valve was deployed, a compliance chamber that simulated pulmonary vascular compliance, and a flow valve to set the pulmonary capillary resistance in order to control the cardiac output or mean flow rate through the fetal heart valve. A working fluid of 60/40 water to glycerin was used as a blood analog to provide a density of  $1,060 \text{ kg/m}^3$  and kinematic viscosity of  $3.5 \times 10^{-6} \text{ m}^2/\text{s}$ . A flow probe (HXL; Transonic Inc., Ithaca, New York) allowed the reading of the average flow rate in the system as well as the flow waveform. The cardiac output was set at 0.5 l/min with a pulmonary artery pressure of 28/4 mm Hg, and the heart rate was set at 90 beats/min (18-20). One hundred consecutive cycles of flow rate and transvalvular pressure gradient (PG), measured using pressure transducers (Validyne Engineering Corp., Northridge, California), were acquired at a sampling frequency of 100 Hz, in accordance with previous studies (16,21,22). From these data, common measures of in vitro valve performance, including effective orifice area (EOA), regurgitant fraction (RF), and pinwheeling index, were computed.

EOA, a measurement of the effective jet area during the phase of the cardiac cycle in which the valve is fully open (23), was calculated based on Gorlin's equation as follows:

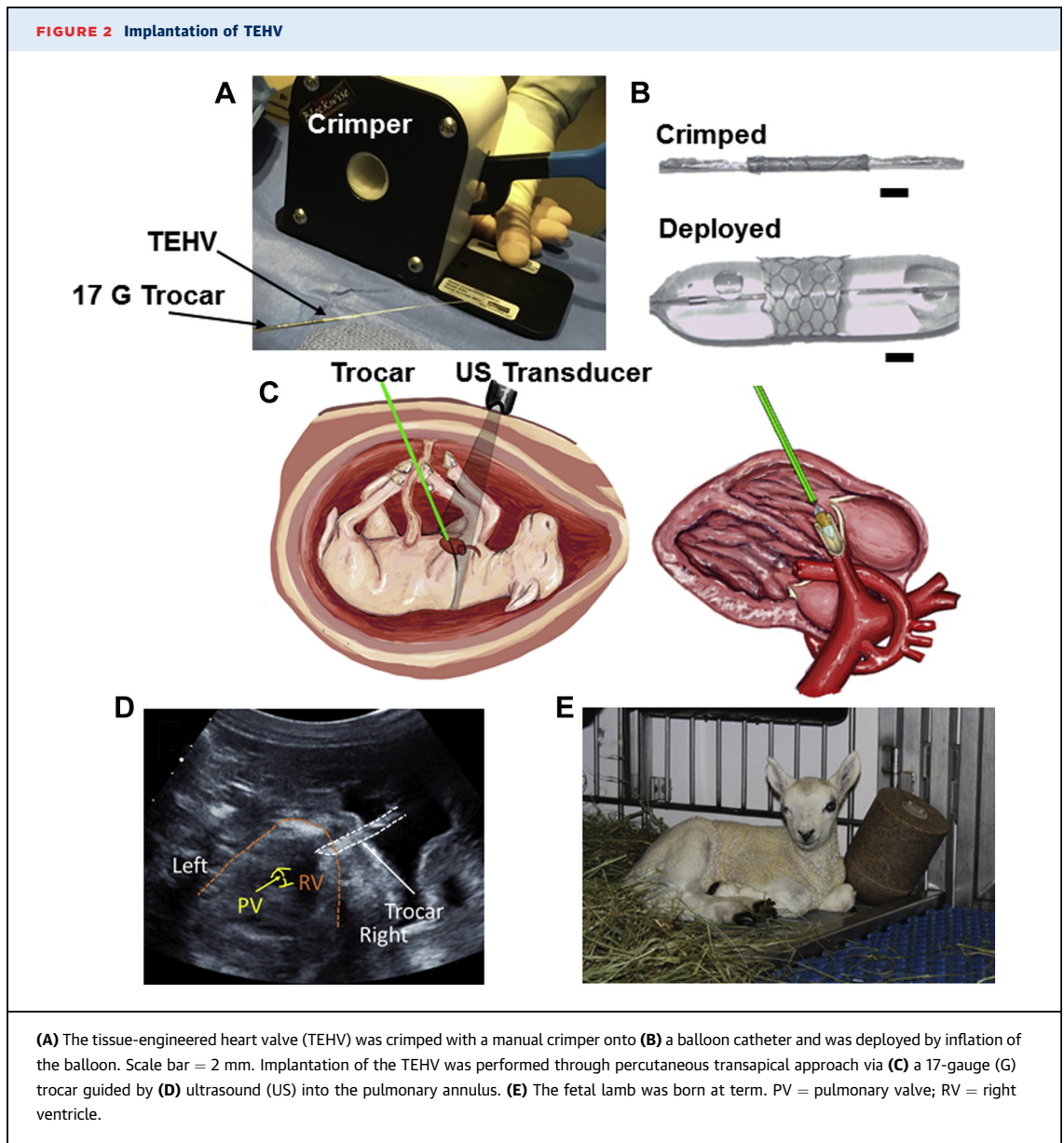
$$EOA = \frac{Q}{51.6\sqrt{PG}} \quad (1)$$

where  $Q$  represents the root mean square pulmonary valve flow ( $\text{cm}^3/\text{s}$ ) and  $PG$  (mm Hg) is the mean transvalvular pressure gradient over a complete cardiac cycle.

The RF was calculated as the ratio of the closing volume (CV) and leakage volume (LV) to the forward flow volume (FV), in accordance with ISO 5840-3 (24):

$$RF = \frac{LV + CV}{FV} \quad (2)$$

Pinwheeling, or localized bending of leaflet material upon closure, is known to cause increased localized bending stresses and hypothesized to correlate with decreased durability (25,26). Ideally, no



pinwheeling or a ratio of 0 is for leaflet and valve durability. The pinwheeling index was computed from en face still frames obtained from high-speed imaging, as per the following equation and in accordance with previous publications (15):

$$PI = \frac{L_{actual} - L_{ideal}}{L_{ideal}} \quad (3)$$

where  $L_{actual}$  represents the deflected free edge of the leaflet in the closed position and  $L_{ideal}$  represents the unconstrained ideal configuration (or shortest possible distance from post and central coaptation region) of the leaflet free edge.

**ANIMAL CARE AND USE.** All procedures were evaluated and approved by the Institutional Animal Care and Use Committee, following humane guidelines as outlined by the National Institutes of Health. Although there are no current large animal models of left or right heart congenital heart disease, pregnant sheep have been shown to be an excellent surrogate for fetal surgical research, owing to similar cardiovascular anatomy and fetal size, compared with humans (27). Pregnant Cheviot ewes between 109 and 115 days gestation (term 145 to 151 days) (28) were used for the study, with 1 to 3 fetuses each. After overnight fasting, the ewes were sedated with

intravenous 5-mg/kg bolus of propofol, placed supine, and intubated. They were ventilated with 100% oxygen and 1% to 2% isoflurane during the procedure.

**FETAL OVINE PERCUTANEOUS TRANSCATHETER PULMONARY VALVE REPLACEMENT.** A custom-made 7 mm × 12 mm TYSHAK Mini Pediatric Valvuloplasty Catheter (NuMED, Hopkinton, New York) was placed over a 0.014 inch × 190 cm Hi-Torque All Star guidewire (Abbott, Abbott Park, Illinois). A Touhy-Borst sidearm adapter was placed on the hub of the balloon catheter. The 0.014-inch wire was marked with 5 cm protruding from the end of the catheter, by securing a torque device behind the Touhy-Borst adapter. The catheter and wire were placed through the outer blunt-tipped cannula of a 17-gauge (outer diameter 1.5 mm) and 15-cm Universal Coaxial Introducer Needle (BD, Franklin Lakes, New York) with the trocar removed, and the catheter was marked with a sterile pen at the point at which the wire was at the tip of the 17-gauge cannula, the point at which the balloon tip was at the tip of the cannula, and the point at which the entire balloon was protruding from the cannula tip. A 10-mm-long zinc alloy stent, with or without the TEHV sewn into it, was crimped on the center of the balloon, without a negative preparation, using a manual crimper on the tightest setting, until the balloon catheter with either the stent or TEHV fit through the 17-gauge cannula without resistance (Figure 2). The 3 facets of the 17-gauge trocar were scraped with a #11 scalpel blade to increase echogenicity.

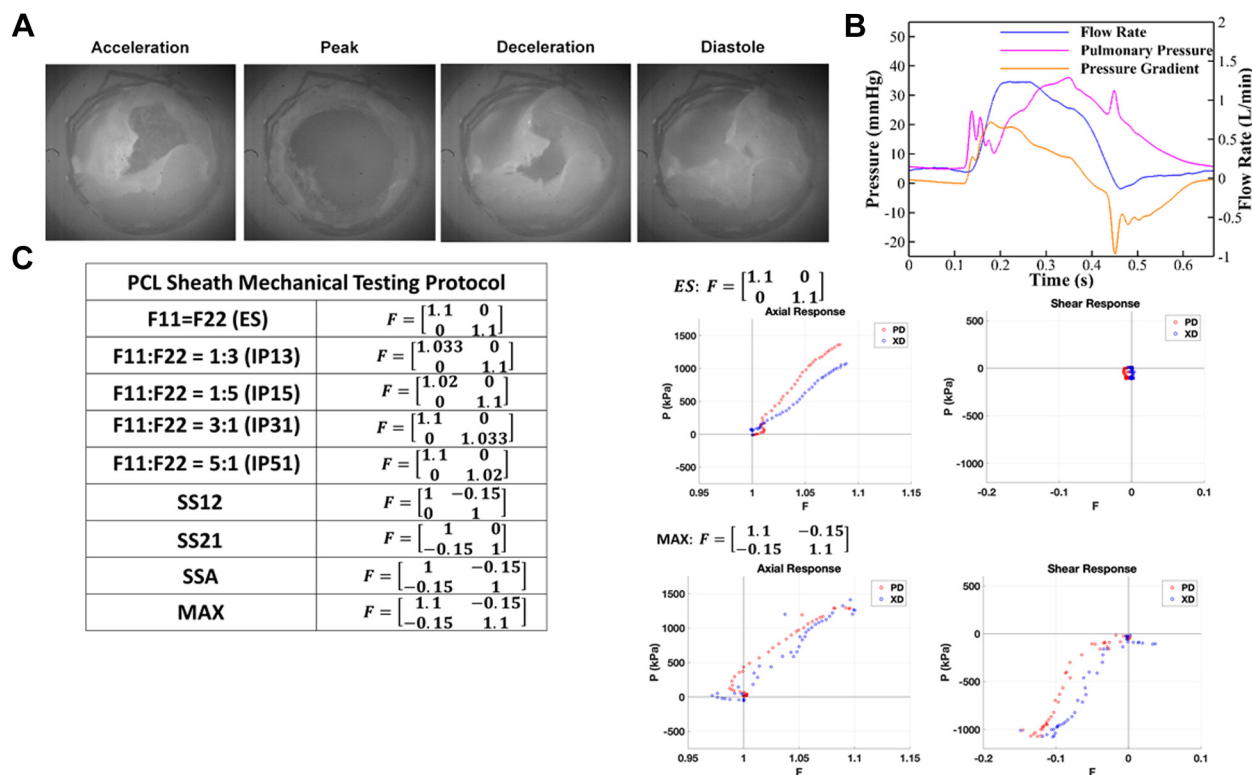
A combination of abdominal fluoroscopy and ultrasound was used to determine the number and locations of the fetuses. Under ultrasound imaging, a 20 gauge × 20 cm Chiba biopsy needle (Cook Medical, Bloomington, Indiana) was inserted into the fetal leg, and an intramuscular injection of fentanyl 50 µg/kg, atropine 20 µg/kg, and vecuronium 200 µg/kg was administered (fetuses were assumed to weigh 1,500 g, based on weights obtained at necropsy). A 22 gauge × 20 cm Chiba biopsy needle was used to test the trajectory needed to enter the fetal right ventricle from the ewe's abdominal wall. The fetal chest was not entered with this needle. In some cases, a small Pfannenstiel (low transverse) incision was made through the pregnant ewe's abdominal wall to allow the obstetrician's hand to manipulate the uterus into proper position for percutaneous fetal RV entrance. The 17-gauge cannula and trocar were introduced percutaneously in the ewe's abdomen, through the uterine wall, and into the chest wall of the fetus under ultrasound guidance. Once in the body of the RV, the trocar was removed, and pulsatile blood return

was confirmed. The wire-balloon-stent or TEHV combination was inserted through the cannula until the wire and then balloon with stent were seen by ultrasound to be crossing the pulmonary valve. In the later cases, as lessons were learned from the developing procedure, prophylactic epinephrine 10 µg/kg was given through the sidearm of the Touhy-Borst into the fetal heart through the lumen of the balloon catheter. When the stent was centered on the pulmonary valve annulus, the balloon was inflated with a commercially available inflation device to 4 atm. The balloon was deflated, and the balloon, wire, and cannula were removed from the ewe completely. The heart was observed for the development of pericardial effusion or bradycardia for approximately 45 min. Enlarging pericardial effusions were treated with needle drainage, and bradycardia was treated with intramuscular or intracardiac epinephrine and atropine. Procedural success was defined as implantation of the zinc stent or TEHV across the pulmonary valve annulus or in the main pulmonary artery (MPA).

**DATA ANALYSIS.** Biaxial mechanical testing and structural characterization data were compiled and analyzed using Tecplot (Tecplot, Bellvue, Washington). Hemodynamic assessment data was compiled and analyzed using MATLAB (The MathWorks, Natick, Massachusetts), as well as Matplotlib and DataGraph graphing software. Gel permeation chromatography data were compiled and analyzed using GraphPad Prism 8.0 (GraphPad Software, San Diego, California). All data presented as mean ± SD.

## RESULTS

**VALVE STRUCTURAL CHARACTERIZATION.** The average tortuosity of the PCL valve material was  $1.13 \pm 0.11$ , indicating a moderate tortuosity level. This measurement is similar to previously reported values of engineered heart valve tissues (29). NOI for the PCL valve material was  $20.7 \pm 7.1\%$ , suggesting slight alignment. A material with slight alignment would likely produce a mildly anisotropic response to equibiaxial strain. This mechanical response can be seen in the biaxial mechanical testing results. There was strong agreement in both tortuosity and NOI between the 2 magnifications, with 20.3% NOI and a tortuosity of 1.12 for the 500× samples and 21.1% NOI and a tortuosity of 1.13 for the 1,000× samples, indicating no dependence on SEM image magnification. The measured fiber density of the PCL valve material is  $0.22 \pm 0.09$ , indicating that the surface layers of the material cover roughly one-fourth of the total area. This measurement takes into account only the

**FIGURE 3** Mechanical Analysis of Tissue-Engineered Heart Valve

(A) En face imaging during the cardiac cycle from acceleration, peak systole, deceleration, and diastole. Full video available in [Video 1](#). (B) Quantification of flow rate, pulmonary pressure, and pressure gradient measured within the flow duplicator. (C) Biaxial mechanical testing using an array of tensile to shear protocols demonstrated that the polycaprolactone (PCL) showed anisotropy toward the primary (circumferential) direction. Representative mechanical testing results shown. ES = equibiaxial strain; F = deformation; IP = in-plane axial strain; MAX = maximum axial and shear strain; P = stress; PD = preferred direction; SS = simple shear (only in one direction); SSA = simple shear all (in both directions); XD = cross-preferred direction.

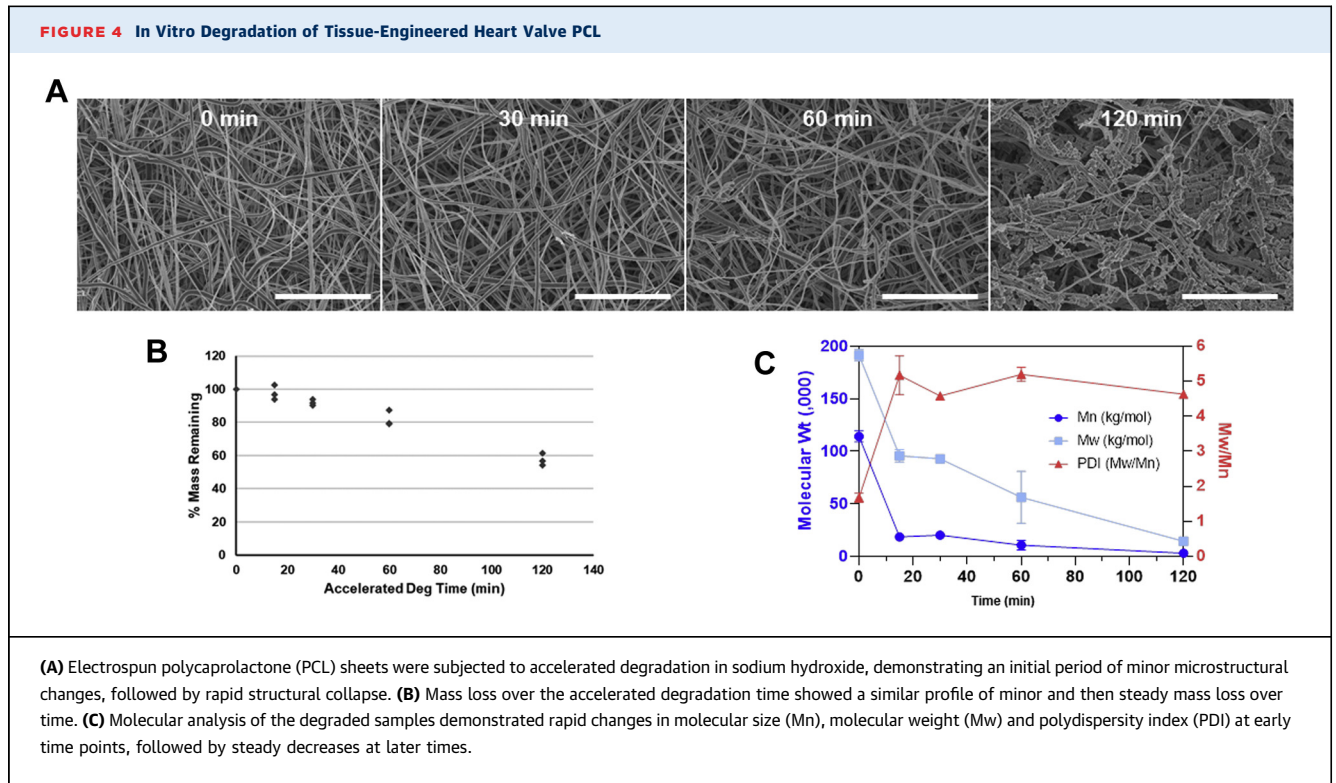
topmost layers of the material, as opposed to all visible layers in a given SEM image.

**VALVE PROPERTIES: MECHANICAL TESTING.** Biaxial mechanical testing of the PCL valve material demonstrated a maximum stress of  $1,357 \pm 116$  kPa in the primary (circumferential) direction and  $1,036 \pm 93$  kPa in the secondary (radial) direction, giving a resulting PD/XD ratio of  $1.32 \pm 0.70$ , representing mild anisotropy with a stronger primary direction. Representative mechanical testing results can be seen in (Figure 3). Anisotropy is desired in engineered heart valve tissues to mimic the anisotropic responses of the circumferential and radial directions of the native valve leaflet (30).

**VALVE PROPERTIES: HEMODYNAMIC ASSESSMENT.** Figure 3 shows the flow rate, pulmonary artery pressure, and transvalvular PG waveforms. The mean PG obtained across the TEHV was  $8.560 \pm 0.139$  mm Hg,

with a peak of 20 mm Hg, and the EOA was  $0.1000 \pm 0.0007$  cm<sup>2</sup>. The RF was  $2.35 \pm 1.99\%$ . Video 1 shows the opening and closing of the valve en face, and Figure 3 shows still frames of the open valve during acceleration, peak, and deceleration phases of the cardiac cycle and the closed valve in diastole. The pinwheeling index obtained with the TEHV was  $0.404 \pm 0.01$ .

**VALVE PROPERTIES: ACCELERATED DEGRADATION.** Accelerated degradation testing on the electrospun PCL valve material demonstrated an initial period of steady mass with a rapid decline in  $M_w$  and  $M_n$  and a corresponding increase in PDI. This initial period was followed by steady mass loss coupled with continued declines in  $M_w$  and  $M_n$  and a relatively stable PDI. By SEM, fiber fractures began to appear in the 60-min samples, while the 120-min samples demonstrated near-complete structural loss (Figure 4).



**DEVELOPMENT OF TRANSCATHETER APPROACH.**

Ten pregnant ewes with 16 fetuses were placed under general anesthesia for development of the percutaneous and fetal percutaneous and transcatheter TEHV procedure (Table 1). Procedures were not attempted on 2 fetuses (#3B, #3C), owing to poor fetal position for intervention.

**Zinc stent implantation.** In order to learn the percutaneous, transcatheter technique, a pilot study using 9 pregnant ewes (#1 to #9) was undertaken, during which zinc stents were implanted in the pulmonary annulus or MPA without a TEHV. Stent implantation was attempted in 12 fetuses and was successful in 5 fetuses. Four of these 5 fetuses had immediate bradycardia, leading to fetal demise, and 2 had an associated pericardial effusion. The only fetus to survive (#8) had the stent implanted in the MPA, instead of across the pulmonary annulus. This fetus survived 6 days and died due to maternal strangulated bowel, as a result of a large laparotomy incision created for fetal positioning. Four of the fetal hearts with stent implants were evaluated by a pediatric cardiac pathologist, and a definitive cause of death was not identified. There was no coronary compression by the stents.

Many changes in technique during the learning curve led to improved success over time and allowed

for 2 subsequent TEHV implantations. For example, fluoroscopy of the ewe’s abdomen at the beginning of the procedure allowed for a faster and more accurate assessment of fetal number and location than with ultrasound alone. Improved success in stent implantation was noted when the RV puncture was anterior in the RV free wall and not close to the apex or posterior through the interventricular septum. As the fetal front legs and hooves often obscured this anterior approach, fetal positioning was critical to the success of the procedure. In addition to the fetal leg anatomy making access to the anterior chest difficult, the flat pregnant abdomen and ewe hip anatomy caused percutaneous access and trajectory barriers that do not exist in the human. If the fetus was not in proper position for an anterior approach into the right ventricle, a small Pfannenstiel incision on the contralateral side of the fetal position, but still between the udders, led to success. A large laparotomy incision lateral to the udder led to strangulation of maternal bowel. The small, medial Pfannenstiel incision allowed the obstetrician’s hand to manipulate the fetus into optimal position through the thin uterine wall. Alternatively, a spinal needle through the ewe’s abdominal wall was often used to manipulate a fetal extremity away from the anterior chest wall. Success was also more common when

**TABLE 1** Implantation Procedure Outcomes

| Fetal Sheep Number* | Gestational Age (Days) | Procedure Attempted       | Pulmonary Valve Annulus by Ultrasound (mm) | Special Technique(s)                | Outcome  | Fetal Weight on Necropsy on Day of Procedure (g) |
|---------------------|------------------------|---------------------------|--|-------------------------------------|--|--|
| 1                   | 109                    | Zinc stent                | 5.7  | None                                | Stent came off balloon, balloon inflated PV, fetal demise                                      | 1,470  |
| 2A                  | 109                    | Zinc stent                | 6.8  | None                                | Stent implanted in PV, complete heart block, fetal demise                                      | 1,340  |
| 2B                  | 109                    | Zinc stent                | 7.1  | None                                | Stent implanted in pericardial space, fetal demise   | 1,315  |
| 3A                  | 115                    | Zinc stent                | 7.1  | Amnioinfusion                       | Stent implanted in PV, bradycardia, pericardial effusion, fetal demise                         | 1,765  |
| 3B                  | 115                    | None, poor fetal position |  | Amnioinfusion                       | Necropsy   | 1,490  |
| 3C                  | 115                    | None, poor fetal position |  | None                                | Necropsy   | 1,515  |
| 4                   | 109                    | Zinc stent                | 6.6  | None                                | Bradycardia with RV puncture, fetal demise   | 1,375  |
| 5                   | 109                    | Zinc stent                | 6.8  | Laparotomy, uterine exteriorization | Cannula entered RV, stent stuck in cannula, bradycardia, fetal demise                          | 1,215  |
| 6                   | 110                    | Zinc stent                | 6.4  | None                                | Stent implanted in pericardial space, fetus survived, necropsy                                 | NA†  |
| 7A                  | 110                    | Zinc stent                | 6.5  | None                                | Cannula entered RV, pericardial effusion, fetal demise   | 1,330  |
| 7B                  | 110                    | Zinc stent                | 6.8  | Laparotomy, intra-abdominal version | Stent implanted in PV, bradycardia, fetal demise   |  |
| 7C                  | 110                    | Zinc stent                | 6.7  | Laparotomy, intra-abdominal version | Balloon inflated in PV, malpositioned on balloon, embolized to RV, necropsy                    | 1,470  |
| 8                   | 110                    | Zinc stent                | 7.0  | Laparotomy, uterine exteriorization | Stent implanted in MPA, fetus survived 6 days, fetal demise due to maternal strangulated bowel | 1,540  |
| 9A                  | 109                    | TEHV in zinc stent        | 6.1  | Laparotomy, intra-abdominal version | TEHV implanted in MPA or PDA, bradycardia, fetal demise  | 1,300  |
| 9B                  | 109                    | Zinc stent                | 6.6  | Laparotomy, intra-abdominal version | Stent implanted in PV, bradycardia and pericardial effusion, fetal demise                      | 1,240  |
| 10                  | 109                    | TEHV in zinc stent        | 6.7  | None                                | TEHV implanted in PV, migrated to MPA, born alive at term                                      | NA†  |

\*Number indicates mother, letter indicates fetus. †Fetus survived and necropsy not on day of procedure.  
MPA = main pulmonary artery; NA = not applicable; PDA = patent ductus arteriosus; PV = pulmonary valve; RV = right ventricle; TEHV = tissue-engineered heart valve.

prophylactic intracardiac epinephrine was administered immediately prior to inflating the balloon. The breed of ewe also may have played a role in survival. Last, minimizing fetal blood loss through the cannula, between the time that the trocar was removed and the balloon or stent were inserted, was critical for fetal survival.

**TEHV implantation.** Using what was learned in the fetal stent pilot study, TEHV implantation was attempted in 2 fetuses (#9A, #10). In fetus #9A, the TEHV was implanted in the MPA, which resulted in obstructed blood flow to the branch pulmonary arteries. Immediate bradycardia was noted, which did not respond to epinephrine. In fetus #10, the TEHV was implanted in the pulmonary annulus. Laminar flow was seen across the TEHV without regurgitation (Figure 5). Subsequent imaging revealed that the stent had migrated to the MPA. The fetus survived the procedure and was born at term gestation. He was alive at 18 months of age.

Success in stent and TEHV implantation improved with time, with 5 of the 7 successful procedures occurring in fetuses #7B, #8, #9A, #9B, and #10. However, bleeding, bradycardia, pericardial effusion,

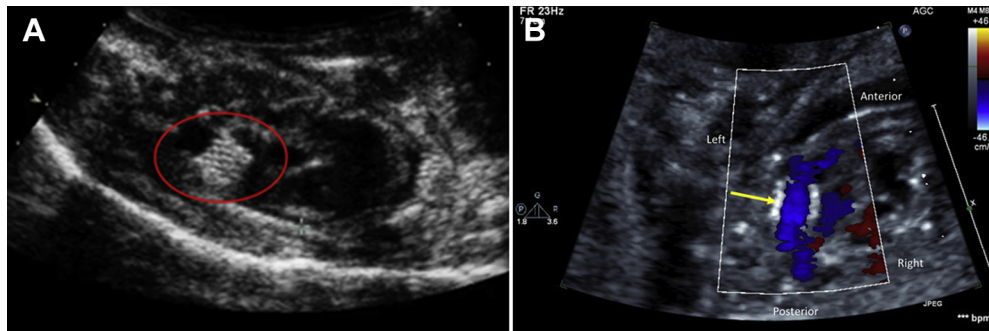
and stent migration represent common serious complications associated with this procedure.

## DISCUSSION

This multidisciplinary work shows the feasibility of replacing the fetal pulmonary valve with a percutaneous, transcatheter, fully biodegradable TEHV. Replacing a stenotic fetal valve with a functional TEHV has the potential to interrupt the development of single-ventricle heart disease by restoring proper flow through the heart. Prenatal treatment provides a potentially curative strategy, as opposed to postnatal palliation of single-ventricle disease, which is fraught with significant morbidity and mortality. Although the various components of the TEHV and the techniques and methods for catheter-based insertion will clearly benefit from further improvements and refinements, establishment of feasibility of this methodology serves as a foundation for future in vitro and in vivo evaluations.

In vitro work on the valve PCL material demonstrated that the designed and created valve was

**FIGURE 5 Successful Delivery of Tissue-Engineered Heart Valve in the Fetal Pulmonary Annulus**



Following (A) successful deployment of a tissue-engineered heart valve (red circle) into the pulmonary annulus of a fetal sheep, (B) laminar flow was detected through the TEHV (yellow arrow) on ultrasound. TEHV = tissue-engineered heart valve.

biodegradable, with a short period of stable mass followed by steady mass loss. Previous studies with similar electrospun PCL material suggest that this degradation is similar to what the valve leaflets will experience over 3 to 4 months in vivo (12). The zinc stent material used has previously been shown, in a rat aortic implantation model, to have no evidence of chronic inflammation, localized necrosis, or progressive intimal hyperplasia, and should retain mechanical integrity to 6 months (11). Although properties of the fetal milieu as an environment for tissue engineering remain to be elucidated, previous studies of tissue engineering topics have demonstrated fetal cells and tissue to have higher regenerative capacity and lower inflammatory responses compared with adult tissues, suggesting that the time frames of degradation of these materials should allow for cellular infiltration and neotissue formation (31).

Biaxial mechanical testing demonstrated that the electrospun PCL was anisotropic, with a stronger circumferential direction. Native heart valve leaflets have been shown to be anisotropic in a similar manner, although the degree of anisotropy in native valves is much higher than that shown in our fetal valve design (32). The maximum stress of the PCL valves was measured at over 1,000 kPa, much higher than the maximum stress experienced by an adult aortic valve in vivo, suggesting that the PCL valve has a suitable strength for in vivo performance without failure (33). Comparison of the microstructural characteristics and mechanical behavior of the PCL material demonstrates the importance of hierarchical design in tissue engineering. The PCL fibers had a

20% alignment toward the circumferential direction, while the mechanical strength of the circumferential direction was 32% higher than the radial direction.

The hemodynamic performance of the TEHV was assessed in a dedicated right heart pulse duplicator. Although no true control valve of similar size is available for comparison, the peak PG reported for the TEHV was 20 mm Hg, while peak PGs reported in children receiving a Melody valve (Medtronic, Minneapolis, Minnesota) or SAPIEN valve (Edwards Lifesciences, Irvine, California) in pulmonary conduits were 13.5 mm Hg (by catheterization at time of implant) and 18.7 mm Hg (by echocardiogram at 1-month follow-up), respectively (34-36). Post-operative pressure gradients of surgical valves implanted in the pulmonary position in pediatric patients (determined by echocardiogram) were reported as 16 to 44 mm Hg (37). The EOA was found to be 35.4% of the available geometric area of the valve. For comparison, a 26-mm SAPIEN 3 aortic valve has been shown to have an EOA of 2.1 cm<sup>2</sup>, roughly 39.6% of its available geometric area based on inflow annular diameter. The mean RF of 2.35% for the TEHV is consistent with trivial pulmonary regurgitation (38,39). The degree of pinwheeling of the TEHV (0.404 ± 0.01) was comparable to that obtained with SAPIEN 3 transcatheter aortic valves (0.122 to 0.366) and thus is indicative of promising leaflet durability (15). In summary, the in vitro evaluation revealed a hemodynamically competent and non-stenotic valve with predicted short-term durability similar to commercially available fixed-tissue transcatheter heart valves. Although the initial hemodynamic evaluation results are promising, further

hemodynamic evaluation at a range of physiological cardiac outputs and heart rates will further inform the future rapid design and development of the TEHV. In addition, future investigation combining the degradation techniques with the hemodynamic evaluations will aid in the understanding of how valve mechanics will change in vivo.

Although many TEHVs have been developed, a lack of mechanistic studies limits the scientific understanding of the mechanisms of neotissue development, as well as clinical success and failure (40). Transcatheter deployment of a tissue-engineered venous valve in a sheep model demonstrated successful function and endothelialization at 2 weeks post-deployment (41). In another study, transcatheter TEHVs, derived from porcine pericardium, were implanted in the subcutaneous tissue of rats and demonstrated limited inflammation and a loss of mechanical properties over the first few weeks post-implantation. These valves, however, were not tested in a functional biological position (42). Development of the large animal model presented in this work will allow for a deeper understanding of these biological mechanisms, as well as the critical design parameters needed to design an ideal TEHV, such as degradation profile and inflammatory status (40).

The bare-metal zinc stent deployments were used to learn the technique of percutaneous, transcatheter implantation into the fetal pulmonary valve annulus, prior to implanting TEHVs. The extremities of the fetal sheep, including the hooves, are typically covering the anterior chest wall access site, making the approach difficult. Manipulation of the extremity away from the chest with a needle percutaneously is often useful. In addition, the pregnant ewe abdomen is flat with the ewe supine, making the approach more difficult than in the human. Furthermore, the fetuses frequently lie under the maternal thighs, which adds complexity. A small Pfannenstiel incision allows the obstetrician to manipulate the fetus into proper position with her hand on the uterus, and this improved success. The valve is still implanted percutaneously through the ewe's abdominal wall, even when the obstetrician is positioning the fetus through the uterine wall. The high rate of fetal death after stent implantation into the pulmonary valve annulus may be due to acute incompetence of the pulmonary valve.

The very low-profile bioabsorbable zinc stent allowed the use of a 17-gauge cannula for the delivery of the TEHV. As large as a 16-gauge needle has been used in human fetal pulmonary balloon valvuloplasty cases (6). Therefore, the smaller 17-gauge needle is an acceptable size for human fetal intervention.

Future work will aim to use this model to evaluate fetal TEHV performance, the development of neotissue development, and stent and valve degradation in vivo.

**STUDY LIMITATIONS.** As there are currently no large animal models of single-ventricle anomalies, all procedures were performed on healthy lambs with presumably normal heart valves. Owing to this, it is difficult to determine if the TEHV is capable of reversing the development of single-ventricle anomalies, as has been recently described in human patients after balloon valvuloplasty. However, the development of this transcatheter fetal technique may still provide many insights into the outcomes related to the stent and valve, as well as the mechanisms of TEHV neotissue development.

Although this pilot study demonstrates the feasibility of performing fetal valve replacement in utero with a TEHV using a percutaneous, catheter-based delivery system, both the prototype and methodology need substantial refinement before translation to the clinic. In fact, the prototype was created from several pre-existing devices which were assembled and used to demonstrate proof of principle rather than to serve as the first-generation product. Further refinement of methods to reduce or even eliminate the morbidity and mortality of in utero fetal cardiac puncture are needed. Significant morbidity and mortality from bleeding, arrhythmias, pericardial effusion, and premature delivery are all possible. In addition, substantial refinements of the biodegradable stent and TEHV scaffold are needed prior to beginning studies to elucidate the cellular and molecular mechanisms of valvular neotissue formation in the fetus, which will ultimately need to be ascertained in order to design and optimize this product. Although degradable stents have the benefit of having a finite life within the body, they also consequently lose mechanical integrity over time. The lifetime of the stent and its changing mechanical properties within the body are critical to the clinical performance of the stent, and stent degradation needs be investigated (43,44). Additionally, while the initial hemodynamic evaluation of the TEHV was promising in its basic function with trivial regurgitation, it is difficult to draw conclusions from measures of valve performance such as EOA and pinwheeling index, owing to the lack of a commercially available size-matched control. Further studies are necessary to assess valve function under a range of hemodynamic parameters and at different time points of degradation in order to inform future TEHV design and development.

Despite these challenges and the nascent stage of this technology, these data support the feasibility of performing percutaneous and transcatheter fetal heart valve replacement and hold extraordinary potential for revolutionizing the treatment and prevention of complex congenital cardiac anomalies.

## CONCLUSIONS

In this work, we have reported the development of a fully bioresorbable valve and stent which can be used for pulmonary valve replacement in utero. We characterized the components of this system in vitro prior to implantation, including accelerated degradation, mechanical, and hemodynamic testing. A percutaneous and transcatheter deployment technique was developed to implant this tissue-engineered valve into a fetal lamb model. The multidisciplinary approach serves as a paradigm for the development of new technologies for translational regenerative medicine, combining the unique expertise of engineers, scientists, and medical specialists for the central goal of improving health outcomes.

**ACKNOWLEDGMENTS** The Animal Resource Core at Nationwide Children's Hospital is thanked for the daily care of the sheep used in this study. Mr. Tim Moran of PediaStent LLC is thanked for his collaboration in providing the zinc alloy stents.

**ADDRESS FOR CORRESPONDENCE:** Dr. Christopher Breuer, Center for Regenerative Medicine, The Abigail Wexner Research Institute at Nationwide Children's Hospital, 700 Children's Drive, WB4154, Columbus, Ohio 43205. E-mail: [christopher.breuer@nationwidechildrens.org](mailto:christopher.breuer@nationwidechildrens.org).

## REFERENCES

1. van der Linde D, Konings EEM, Slager MA, et al. Birth prevalence of congenital heart disease worldwide: a systematic review and meta-analysis. *J Am Coll Cardiol* 2011;58:2241-7.
2. Breuer CK, Mettler BA, Anthony T, Sales V, Schoen FJ, Mayer JE. Application of tissue-engineering principles toward the development of a semilunar heart valve substitute. *Tissue Eng* 2004;10:1725-36.
3. Armstrong AK, Berger F, Jones TK, et al. Association between patient age at implant and outcomes after transcatheter pulmonary valve replacement in the multicenter Melody valve trials. *Catheter Cardiovasc Interv* 2019;94:607-17.
4. François K, De Groot K, Vandekerckhove K, De Wilde H, De Wolf D, Bové T. Small-sized conduits in the right ventricular outflow

- tract in young children: bicuspidized homografts are a good alternative to standard conduits. *Eur J Cardiothorac Surg* 2018;53:409-15.
5. Huygens SA, Rutten-van Mölken MPMH, Noruzi A, et al. What is the potential of tissue-engineered pulmonary valves in children? *Ann Thorac Surg* 2019;107:1845-53.
6. Tulzer A, Arzt W, Gitter R, Prandstetter C, Grohmann E, Mair R, Tulzer G. Immediate effects and outcome of in-utero pulmonary valvuloplasty in fetuses with pulmonary atresia with intact ventricular septum or critical pulmonary stenosis. *Ultrasound Obstet Gynecol* 2018;52:230-7.
7. Weber B, Emmert MY, Behr L, et al. Prenatally engineered autologous amniotic fluid stem cell-

- based heart valves in the fetal circulation. *Biomaterials* 2012;33:4031-43.
8. Miller DC, Blackstone EH, Mack MJ, et al. PARTNER Trial Investigators and Patients; PARTNER Stroke Substudy Writing Group and Executive Committee. Transcatheter (TAVR) versus surgical (AVR) aortic valve replacement: occurrence, hazard, risk factors, and consequences of neurologic events in the PARTNER trial. *J Thorac Cardiovasc Surg* 2012;143:832-43.e13.
9. Petit CJ. Pediatric transcatheter valve replacement: guests at our own table? *Circulation* 2015;131:1943-5.
10. Botelho RD, Imada V, Rodrigues da Costa KJ, et al. Fetal myelomeningocele repair through a mini-hysterotomy. *Fetal Diagn Ther* 2017;42:28-34.

## PERSPECTIVES

**COMPETENCY IN MEDICAL KNOWLEDGE:** We created a fully biodegradable fetal valve and stent, using tissue engineering methods, that was deployed in the fetal ovine pulmonary annulus with a percutaneous and transcatheter approach. Valves were made of electrospun PCL and mounted on degradable zinc-aluminum alloy stents. They were analyzed in vitro through accelerated degradation, mechanical, and hemodynamic testing. The hemodynamic performance of the TEHV in a right heart pulse duplicator showed a peak pressure gradient of 20 mm Hg, which is comparable to gradients obtained in transcatheter heart valves placed in children. The valve had a regurgitant fraction indicative of only trivial regurgitation. The very low-profile valve was successfully implanted in a fetal lamb through a 17-gauge cannula percutaneously, and the fetus was delivered alive at term. This work showcased the importance of a large, multidisciplinary team in solving multifaceted medical problems. Development of our successful stent, valve, and delivery technique would not have been possible without the combined work of many clinicians, scientists, and engineers.

**TRANSLATIONAL OUTLOOK:** We showed the feasibility of implanting a fully biodegradable TEHV into a fetal large animal model using only a 17-gauge needle. This study laid the groundwork for investigating the regenerative capacity of the fetal milieu for neovalve formation. Future work will use this model to evaluate fetal TEHV performance, the development of neotissue development, and stent and valve degradation in vivo. Fetal TEHV implantation has the potential to interrupt the development of congenital heart disease in utero and to promote a biventricular circulation by replacing abnormal valves and improving flow dynamics. Such a low-profile biodegradable valve also has great potential for transcatheter implantation in infants, which is not possible with current technology.

11. Bowen PK, Guillory RJ 2nd, Shearier E, et al. Metallic zinc exhibits optimal biocompatibility for bioabsorbable endovascular stents. *Mater Sci Eng C Mater Biol Appl* 2015;56:467-72.
12. Lee KW, Gade PS, Dong L, et al. A biodegradable synthetic graft for small arteries matches the performance of autologous vein in rat carotid arteries. *Biomaterials* 2018;181:67-80.
13. Kim H, Sung SC, Chang YH, et al. A new simplified technique for making tricuspid expanded polytetrafluoroethylene valved conduit for right ventricular outflow reconstruction. *Ann Thorac Surg* 2013;95:e131-3.
14. Sacks MS, Smith DB, Hiester ED. A small angle light scattering device for planar connective tissue microstructural analysis. *Ann Biomed Eng* 1997;25:678-89.
15. Hatoum H, Yusefi A, Lilly S, Maureira P, Crestanello J, Dasi LP. An in vitro evaluation of turbulence after transcatheter aortic valve implantation. *J Thorac Cardiovasc Surg* 2018;156:1837-48.
16. Hatoum H, Dollery J, Lilly SM, Crestanello, Dasi LP. Sinus hemodynamics variation with tilted transcatheter aortic valve deployments. *Ann Biomed Eng* 2019;47:75-84.
17. Hatoum H, Gooden S, Heitkemper M, et al. Fetal transcatheter trileaflet heart valve hemodynamics: implications of scaling on valve mechanics and turbulence. *Ann Biomed Eng* 2020;48:1683-93.
18. Hamill N, Yeo L, Romero R, et al. Fetal cardiac ventricular volume, cardiac output, and ejection fraction determined with 4-dimensional ultrasound using spatiotemporal image correlation and virtual organ computer-aided analysis. *Am J Obstet Gynecol* 2011;205:76.e1-10.
19. De Smedt MC, Visser GH, Meijboom EJ. Fetal cardiac output estimated by Doppler echocardiography during mid- and late gestation. *Am J Cardiol* 1987;60:338-42.
20. Skinner JR, et al. Pulmonary and systemic arterial pressure in hyaline membrane disease. *Arch Dis Child* 1992;67:366-73.
21. Yap C, Saikrishnan N, Yoganathan AP. Experimental measurement of dynamic fluid shear stress on the ventricular surface of the aortic valve leaflet. *Biomech Model Mechanobiol* 2012;11:231-44.
22. Hatoum H, Maureira P, Dasi LP. A turbulence in vitro assessment of On-X and St Jude Medical prostheses. *J Thorac Cardiovasc Surg* 2020;159:88-97.
23. Dasi LP, Simon HA, Sucusky P, Yoganathan AP. Fluid mechanics of artificial heart valves. *Clin Exp Pharmacol Physiol* 2009;36:225-37.
24. ISO 5840-3:2013. Cardiovascular implants – Cardiac valve prostheses – Part 3: heart valve substitutes implanted by transcatheter techniques. Geneva, Switzerland: International Organization for Standardization, 2013.
25. Martin C, Sun W. Simulation of long-term fatigue damage in bioprosthetic heart valves: effects of leaflet and stent elastic properties. *Biomech Model Mechanobiol* 2014;13:759-70.
26. Doose C, Kütting M, Egron S, et al. Valve-in-valve outcome: design impact of a pre-existing bioprosthesis on the hydrodynamics of an Edwards Sapien XT valve. *Eur J Cardiothorac Surg* 2017;51:562-70.
27. Park HK, Park YH. Fetal surgery for congenital heart disease. *Yonsei Med J* 2001;42:686-94.
28. Anderson GB, Bradford GE, Cupps PT. Length of gestation in ewes carrying lambs of two different breeds. *Theriogenology* 1981;16:119-29.
29. Eckert CE, Mikulis BT, Gottlieb D, et al. Three-dimensional quantitative micromorphology of pre- and post-implanted engineered heart valve tissues. *Ann Biomed Eng* 2011;39:205-22.
30. Hasan A, Ragaert K, Swieszkowski W, et al. Biomechanical properties of native and tissue engineered heart valve constructs. *J Biomech* 2014;47:1949-63.
31. Turner CG, Fauza DO. Fetal tissue engineering. *Clin Perinatol* 2009;36:473-488, xii.
32. Stella JA, Sacks MS. On the biaxial mechanical properties of the layers of the aortic valve leaflet. *J Biomech Eng* 2007;129:757-66.
33. Thubrikar M, Piepgrass WC, Deck JD, Nolan SP. Stresses of natural versus prosthetic aortic valve leaflets in vivo. *Ann Thorac Surg* 1980;30:230-9.
34. Zhang B, Chen X, Xu TY, et al. Transcatheter pulmonary valve replacement by hybrid approach using a novel polymeric prosthetic heart valve: proof of concept in sheep. *PLoS One* 2014;9:e100065.
35. Gillespie MJ, McElhinney DB, Kreutzer J, et al. Transcatheter pulmonary valve replacement for right ventricular outflow tract conduit dysfunction after the Ross procedure. *Ann Thorac Surg* 2015;100:996-1003.
36. Kenny D, Hijazi ZM, Kar S, et al. Percutaneous implantation of the Edwards SAPIEN transcatheter heart valve for conduit failure in the pulmonary position: early phase 1 results from an international multicenter clinical trial. *J Am Coll Cardiol* 2011;58:2248-56.
37. Gulack BC, Benrashed E, Jaquiss RDB, Lodge AJ. Pulmonary valve replacement with a Trifecta valve is associated with reduced trans-valvular gradient. *Ann Thorac Surg* 2017;103:655-62.
38. Nishimura RA, Otto CM, Bonow RO, et al. 2014 AHA/ACC guideline for the management of patients with valvular heart disease: a report of the American College of Cardiology/American Heart Association Task Force on Practice Guidelines. *J Am Coll Cardiol* 2014;63:e57-185.
39. Mercer-Rosa L, Ingall E, Zhang X, et al. The impact of pulmonary insufficiency on the right ventricle: a comparison of isolated valvular pulmonary stenosis and tetralogy of Fallot. *Pediatr Cardiol* 2015;36:796-801.
40. Blum K, Drews J, Breuer CK. Tissue engineered heart valves: a call for mechanistic studies. *Tissue Eng Part B Rev* 2018;24:240-53.
41. Syedain ZH, Jenson AC, Patel PS, et al. Tissue-engineered transcatheter vein valve. *Biomaterials* 2019;216:119229.
42. Khorramirouz R, Go JL, Noble C, Morse D, Lerman A, Young MD. In vivo response of acellular porcine pericardial for tissue engineered transcatheter aortic valves. *Sci Rep* 2019;9:1094.
43. Welch TR, Nugent AW, Veeram Reddy SR. Biodegradable stents for congenital heart disease. *Interv Cardiol Clin* 2019;8:81-94.
44. Borhani S, Hassanajili S, Tafti SHA, Rabbani S. Cardiovascular stents: overview, evolution, and next generation. *Prog Biomater* 2018;7:175-205.

---

**KEY WORDS** congenital heart disease, tissue-engineered heart valve, transcatheter heart valve, translational medicine

---

**APPENDIX** For a supplemental video, please see the online version of this paper.